Journal of Solid State Chemistry **155,** 105–111 (2000)
doi:10.1006/jssc.2000.8909, available online at http://www.idealibrary.com on IDEAL®

Interactions of Sliding Charge-Density Waves with Phonons

J. W. Brill, B. M. Emerling, and X. Zhan

Department of Physics and Astronomy, University of Kentucky, Lexington, Kentucky 40506-0055

Received May 16, 2000; in revised form July 25, 2000; accepted August 2, 2000

DEDICATED TO PROFESSOR J. M. HONIG

While it is well known that the depinning of a charge-density wave (CDW) in a quasi-one-dimensional conductor causes unusual electron transport properties, it also affects the lattice phonons in surprising ways. In this paper, we discuss two such effects. In orthorhombic TaS_3, depinning causes low-frequency acoustic velocities to decrease, presumably because the local phase of the CDW can relax in an oscillating strain when it is depinned. We have used torsional oscillator measurements to determine the voltage dependence of the average relaxation time. In monoclinic $K_{0.3}MoO_3$, we have measured changes in the frequencies, oscillator strengths, and bandwidths of optic phonons near current contacts. The sign of these changes depends on the polarity of the current, indicating that they are due to polarization of the CDW which accompanies depinning.

Key Words: **blue bronze; TaS_3; charge-density wave; elastic; phonons; electrooptic; electromechanical; internal friction; shear compliance; infrared.**

1. INTRODUCTION

During the past two decades, there has been considerable interest in inorganic quasi-one-dimensional metals which exhibit charge-density wave (CDW) ground states (1). Much of this interest has been focused on the unusual electronic properties associated with depinning of the CDW, including strongly non-Ohmic conductivity, memory effects, and ac voltage generation by dc currents (2). However, the depinning of the CDW also affects the host lattice. In this paper, we will review some of our recent results on the consequences of CDW depinning on phonons in TaS_3 and $K_{0.3}MoO_3$, two of the best-studied CDW materials.

A metal is called quasi-one-dimensional if the orbitals of the conduction band (usually "d" orbitals for an inorganic crystal) have much greater overlap in one crystallographic direction than in the other two, resulting in parallel sheets of Fermi surface at $\pm k_F$. Such a nested Fermi surface is subject to a Peierls distortion: a superlattice forms with wavevector $Q = 2k_F$, gaps open at the Fermi surface, and the electron density becomes modulated (2),

$$\rho = \rho_0 + \rho_{CDW} \cos(Qz + \phi), \qquad [1]$$

where z is the conducting chain direction, and ρ_{CDW} and $\phi(\mathbf{r}, t)$ are, respectively, the amplitude and local phase of the CDW. In inorganic materials, Peierls transitions typically occur at $T_c \approx 100$ K (1, 2).

For an incommensurate Q in a perfect crystal, the phase will have no preferred value and the CDW will be free to move through the crystal. However, in the presence of impurities, the phase varies spatially to minimize the CDW potential energy. For small applied voltages, the phase will remain in this "pinned" configuration, but if the voltage exceeds a threshold, V_P (typically proportional to the square of the impurity concentration), the CDW "slides," carrying collective current and giving rise to the unusual electron transport properties of these materials (2).

Early measurements (3–7) of effects of depinning on phonons used mechanical resonances to probe changes in elastic constants, proportional to the squares of the velocities of long wavelength acoustic phonons. For most CDW materials, it was found that the Young's modulus and shear modulus decreased when the CDW became depinned (3–8). These changes depended strongly on experimental conditions, including the frequency of the oscillation, suggesting that they were relaxational in origin (3, 9–12). In Section 2, we will discuss our recent measurements of the very low frequency shear compliance of TaS_3, used to determine the voltage dependence of the average elastic relaxation time.

We have recently observed that optical phonons are also affected by CDW depinning (13). Unlike the acoustic modes, the changes in optic modes depend on sample polarity and therefore are probably caused by changes in CDW polarization, which accompany depinning. In Section 3, we will describe the changes in optical phonons observed in blue bronze, using infrared transmission spectroscopy.

2. SHEAR COMPLIANCE OF TaS_3

Crystals of TaS_3 (14) grow as thin fibers; while they can be over 1 cm long in the high conductivity (c) direction, they

0022-4596/00 $35.00

are typically $\leq 10\,\mu m$ in the transverse directions. The orthorhombic polytype (o-TaS_3) undergoes a Peierls transition into a semiconducting CDW state at $T_c = 220$ K (14), below which it exhibits all the novel electronic properties associated with sliding CDWs, with typical threshold electric fields (in nominally pure samples) $\approx \frac{1}{4}$ V/cm (2).

Measurements on mechanical resonances of o-TaS_3 near 1 kHz showed that the shear (5) and Young's (3, 4) moduli decreased, by ≈ 20 and 2%, respectively, at voltages above V_P (e.g., see Fig. 1). The quality factors of the resonances also decreased above threshold, indicating increased internal friction when the CDW was sliding (3–5). The magnitude of the decrease in Young's modulus diminishes with increasing elastic frequency (9), and much smaller anomalies ($<0.1\%$) are observed at ultrasonic frequencies (15).

It was suggested that the elastic changes are relaxational in origin, with an average relaxation time that increases as the voltage approaches threshold from above: when the CDW is pinned, some property of it is not able to relax to the changing strain, but it is able to relax when depinned (3, 10, 12, 15). The inset to Figure 3 shows a dispersion curve for an acoustic phonon in the case of a wavevector-independent average relaxation time (τ_0); the slope (i.e., the phonon velocity, proportional to the square root of the corresponding elastic modulus) increases when the frequency becomes larger than $1/\tau_0$.

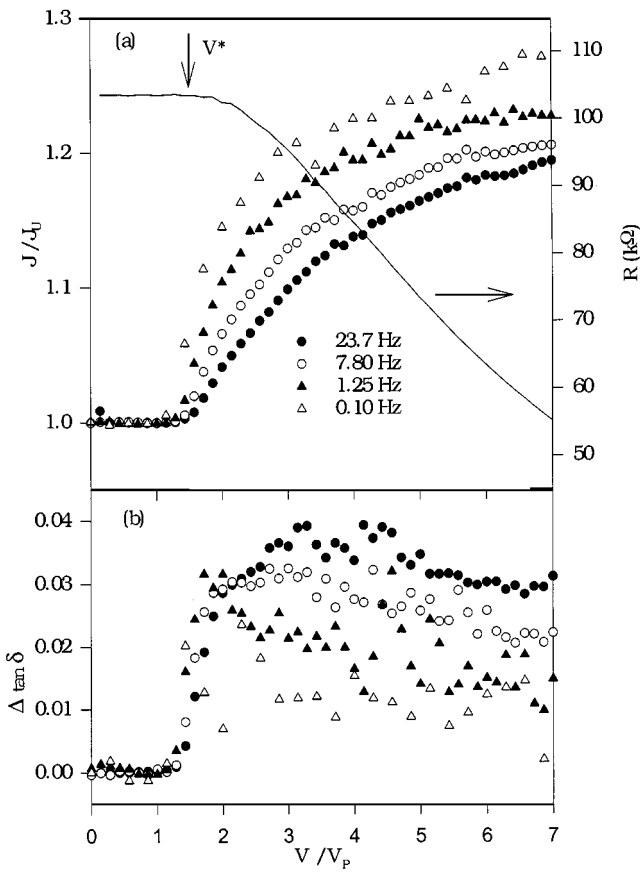

FIG. 1. Shear compliance (a) and internal friction (b) vs voltage for a crystal of TaS_3 at 85 K at a few elastic frequencies. The threshold voltage $V_P = 70$ mV. Also shown is the voltage dependence of the dc resistance; V^* is the onset of non-Ohmic resistance, i.e., sliding of the CDW into the contacts (11).

In particular, Mozurkewich considered the modulus changes that would result from relaxation of the local CDW phase (12). In general, ϕ varies spatially as a consequence of the competition between impurity pinning and the CDW's intrinsic periodicity (2). If the latter depends on crystal strain, reflecting a strain dependent Fermi surface (5, 11, 12), the optimum phase will also be strain dependent. However, if $\phi(\mathbf{r})$ remains pinned below threshold, the elastic moduli at low voltages will be greater than at high voltages, where ϕ can relax. For example, the shear modulus will decrease by

$$\Delta G = -K_{CDW}\,[\partial \ln (k_F)/\partial \varepsilon]^2, \qquad [2]$$

when the CDW becomes depinned (11, 12). Here, ε is torsional strain and K_{CDW} is the (longitudinal) rigidity of the CDW. The 20% anomalies in G for TaS_3 imply that $[\partial \ln (k_F)/\partial \varepsilon]^2 \approx 1$ (11). While this model seemed able to account for several qualitative aspects of the elastic anomalies (10, 12), it was clear that a wide distribution of relaxation times was needed to account for the magnitudes and frequency dependences of the modulus and internal friction anomalies (3, 15).

In recent work, we attempted to study the distribution of time constants and its possible divergence at V_P by measuring the low-frequency shear compliance, $J \equiv 1/G = \varepsilon/\sigma$, where σ is the torsional stress (11). These measurements were done by mounting the crystal as a torsional oscillator, with a small magnetized steel wire glued to the center of the sample as the inertial element. Oscillating torque ($\propto \sigma$) was applied by an ac magnetic field from Helmholtz coils surrounding the sample. The sample's twist angle ($\propto \varepsilon$) was measured by changes in the response of a radio frequency cavity containing the sample (16). While the magnitude of the compliance is proportional to the twist angle for fixed torque, the internal friction equals the tangent of the phase difference between strain and stress, δ (11).

The voltage dependence of the dc resistance, J (normalized to its low voltage, i.e., unrelaxed, value J_U) and internal friction for a o-TaS_3 crystal at 85 K are shown in Fig. 1 (11). The compliance and internal friction are shown for a few, representative elastic frequencies. The drop in resistance with increasing voltage is indicative of the sliding CDW. The compliance slowly increases by $\approx 25\%$ (i.e., G decreases by 20%) as V increases above V_P, defined here as the onset of the elastic anomalies; the internal friction rises rapidly above V_P, reaching a maximum value (of a few percent) near $2V_P$. However, the changes remain frequency dependent down to the lowest frequencies, indicative of the

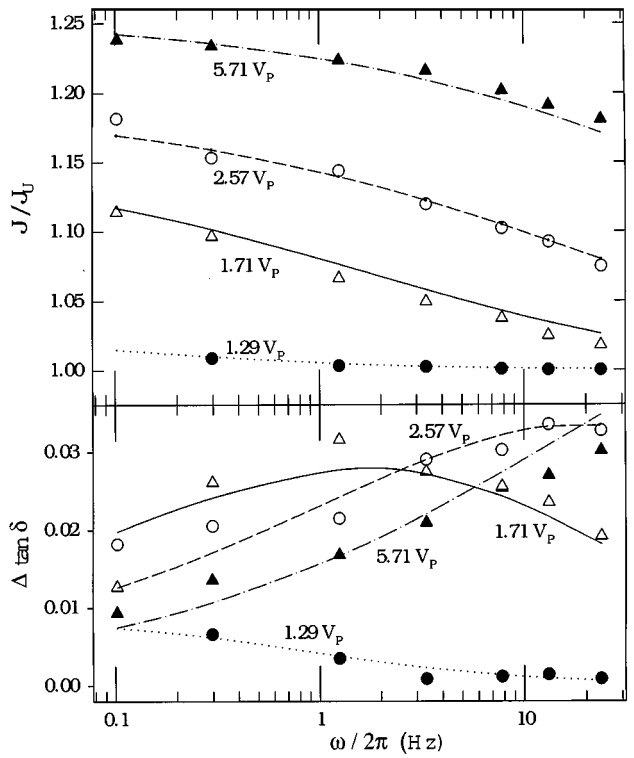

FIG. 2. Shear compliance and internal friction as functions of frequency at several voltages. The curves show the fits to Eq. [3]. Note that the symbols are the same in both panels.

slow dynamics associated with depinning. For this sample, the threshold voltage ($V_P = 70$ mV) corresponds to a threshold electric field of ≈ 0.2 V/cm and an impurity concentration of ≤ 300 ppm.

Note that the elastic threshold, V_P, is slightly below V^*, which we define to be the voltage at which we can observe changes in resistance. This difference suggests that the CDW is more strongly pinned at the electrical contacts than in the bulk of the sample; for $V_P < V < V^*$, the CDW polarizes between the contacts (13, 17).

By taking "vertical slices" of voltage dependent data at several frequencies, one can survey the frequency dependence of the compliance and internal friction, as shown in Fig. 2. At a given voltage above threshold, the compliance decreases logarithmically with frequency (18), indicative of a large distribution of relaxation times, and the internal friction peak moves to higher frequencies, i.e., smaller average time constants, with increasing voltage, as expected.

We have analyzed the elastic anomalies by fitting the complex compliance, $\mathbf{J} \equiv J \exp(i\delta)$ to

$$\mathbf{J}/J_U = 1 + j\,(V)/\{1 + [i\omega\tau_0(V)]^{1-\alpha}\}^{\beta}, \qquad [3]$$

where j and τ_0 are the relative relaxation strength and average relaxation time at voltage V. This expression was introduced to fit the dielectric constant of polymers (19) and has also been used to fit the dielectric constants of CDW materials (2). For simple Debye relaxation (i.e., a single relaxation time), $\alpha = 0$ and $\beta = 1$; other exponents indicate a distribution of Debye relaxation times (20). In principle, α, β, j, and τ_0 may all be voltage dependent, but the scatter in our data precluded obtaining meaningful fits allowing all four to vary. For simplicity, we took α and β as independent of voltage, and found that the complex compliance could be roughly fit with $\alpha = 0.64$ and $\beta = 2.75$ (11), corresponding to a three-decade-wide distribution of relaxation times (21). The values of J/J_U and $\tan\delta$ calculated from these fits are shown by the curves in Fig. 2. (The fits of the internal friction are poorer than those of the compliance, reflecting the noise in the low-frequency internal friction data as well as the insensitivity of Re**J** to δ.)

The fitted values of j(V) and τ_0 (V) are shown in Fig. 3. The voltage dependence of j suggests that the fraction of the sample relaxing grows with voltage, but this may be a consequence of our assumption of constant α and β, i.e., constant (normalized) distribution of relaxation times. However, the stronger voltage dependence of the average relaxation time, $\tau_0 \propto (V - V_P)^{-3}$, is less sensitive to the choice of fitting function, and suggests that depinning can be considered a dynamic critical transition (22), although it is certainly not clear if we are yet in a critical regime of voltage. Future measurements will address these issues.

Above 1 kHz, the frequency dependence of the elastic anomalies is believed to become much stronger than the logarithmic dependence shown in Fig. 2; for example,

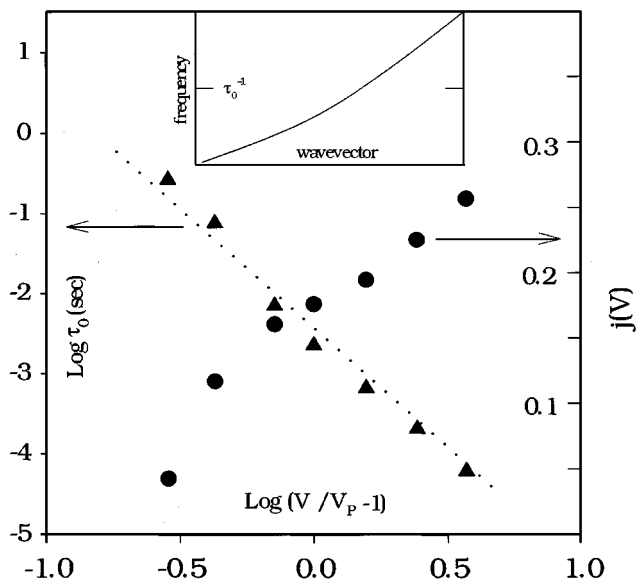

FIG. 3. Voltage dependence of the average relaxation time and relative relaxation strength determined from the fits to Eq. [3]. The dotted line has slope = − 3. (Inset) A phonon dispersion curve when modified by relaxation, with average relaxation time τ_0.

the Young's modulus anomaly $\propto \omega^{-3/4}$ (9), extrapolating to the small anomalies observed ultrasonically (15). Hence, one would expect changes at infrared frequencies to be unobservable. However, large changes ($>1\,\mathrm{cm}^{-1}$) with CDW depinning in the frequency and linewidth of a Raman active phonon in TaS_3 have been reported (23). Working with another quasi-one-dimensional CDW conductor, $K_{0.3}MoO_3$, we have observed much smaller, polarity-dependent changes in the frequency, width, and oscillator strength of optical phonons (13).

3. ELECTROMODULATED INFRARED TRANSMISSION SPECTRUM OF $K_{0.3}MoO_3$

$K_{0.3}MoO_3$ ("blue bronze") has a monoclinic structure with sheets of edge-sharing MoO_6 octahedra, in [010]–[102] planes, separated by K^+ ions. The sheets are uninterrupted along b, the high conductivity direction; the transverse conductivity is two orders of magnitude lower, and blue bronze has properties representative of quasi-one-dimensional conductors (24). In particular, it undergoes a Peierls transition into a CDW state at $T_c = 180$ K, below which it exhibits most of the unusual electronic properties associated with sliding CDWs (2, 24).

The [010]–[102] planes are natural cleavage planes, and crystals can be cleaved with sticky tape to thicknesses $d < 10\,\mu\mathrm{m}$. While these thin plates are still optically thick for light polarized along b, they are translucent (i.e., $\alpha d \approx 1$, where α is the absorptivity) in the infrared for light polarized along [102], so transmission spectra can be taken.

We have recently found that the IR transmission (T) is affected by CDW depinning. Neglecting multiple internal reflections, $T = (1 - R)^2 \exp(-\alpha d)$, where R is the reflectivity, so that

$$\Delta T/T = -2\Delta R/(1 - R) - d\Delta\alpha. \qquad [4]$$

For photon energies below the estimated value of the gap ($v_{\mathrm{gap}} \approx 1400\,\mathrm{cm}^{-1}$ (25)), the transmission increases on the positive side of the sample and decreases on the negative (13, 17, 26). (In contrast, no polarity dependence was observed for the low-frequency elastic anomalies (3).) The polarity dependence of ΔT suggested that it is caused by CDW polarization, $\partial\phi/\partial z$, which accompanies depinning (27). Application of a voltage larger than threshold causes the CDW to become compressed at the positive contact and rarefied at the negative contact. The density of the CDW condensate is two electrons *per wavelength* per chain, so that compressions (rarefactions) are negatively (positively) charged (28). A detailed examination of the spatial dependence of the electromodulated transmission showed that $\Delta T/T \propto \partial\phi/\partial z$ (17). (As for the elastic anomalies, the infrared changes have an onset at a voltage V_P below V^*, the onset for non-Ohmic conductance, indicating that the anomalies require only that the CDW be depinned in the bulk, and not that it can slide into the contacts.)

The transmission changes for all frequencies below the gap. This unusually broad electrooptic spectral response suggested that it is essentially associated with the *intraband* absorption of quasiparticles thermally excited out of the CDW, and indeed we found that $\Delta T/T$ is thermally activated below 110 K (13, 25). In blue bronze, the dominant mobile quasiparticles are electrons (29). These will become rarefied (compressed) at the positive (negative) contacts to screen the CDW deformations (28); hence intraband absorption will decrease at the positive contact and increase at the negative, as we observe.

Intraband quasiparticle absorption would result in a featureless $\Delta T/T$ spectrum for photon energies (v) below the CDW gap. Figure 4 shows the $\Delta T/T$ spectrum and the corresponding absorption spectrum, plotted as the optical density $[-\ln(T)]$, measured simultaneously on a $K_{0.3}MoO_3$ sample at 82 K (13). For these spectra, the transmission was measured through a 160-μm-wide slit behind the sample adjacent to a current contact. Tunable diode lasers were used as light sources. The lasers were not mode selected and the typical spectral bandwidth was $\approx 10\,\mathrm{cm}^{-1}$. A symmetric square wave voltage, $V = \pm V^* = \pm 1.7\,V_P$ was applied to the ($\approx$1-mm-long) sample, and the modulated transmission measured with a lock-in amplifier, so that $\Delta T \equiv [T(+V^*) - T(-V^*)]$. Details of the experimental technique are given in Ref. 13. Note that, within our resolution, the normalized spectrum is independent of the applied voltage: $\Delta T(v, V)/T = S(v)\,F(V)$. (For this sample, $V_P = 15$ mV, corresponding to a threshold electric field of ≈ 150 mV/cm and a small impurity concentration of ≤ 300 ppm (2).)

The increase in absorption for $v > 1050\,\mathrm{cm}^{-1}$ is associated with excitations across the CDW gap, broadened by quantum and thermal fluctuations (25). The increase in transmission at the positive contact for $v < v_{\mathrm{gap}}$, resulting from the decrease in quasiparticle concentration, is expected to be replaced by an increase in interband absoprtion and hence a sign change in $\Delta T/T$ for $v > v_{\mathrm{gap}}$. Therefore, $|\Delta T/T|$ decreases as v approaches v_{gap} (13).

For $v < 1050\,\mathrm{cm}^{-1}$, $\Delta T/T$ has an average value $\approx 0.15\%$. However, this "plateau" is strongly modulated by changes associated with the phonon absorption lines, indicated by the peaks in the optical density. This structure in $\Delta T/T$ shows that these phonons are affected by polarization of the CDW. (Because of the complexity of the unit cell, the distortion coordinates of most phonons are not known (30).) Changes in phonon spectra can be described in terms of changes in the oscillator strength, frequency, and/or bandwidth. In fact, the $\Delta T/T$ spectral shape for each phonon can be characterized as primarily resulting from one of these properties, but changes of all three types are observed. (Note that both terms in Eq. [4] will give similar

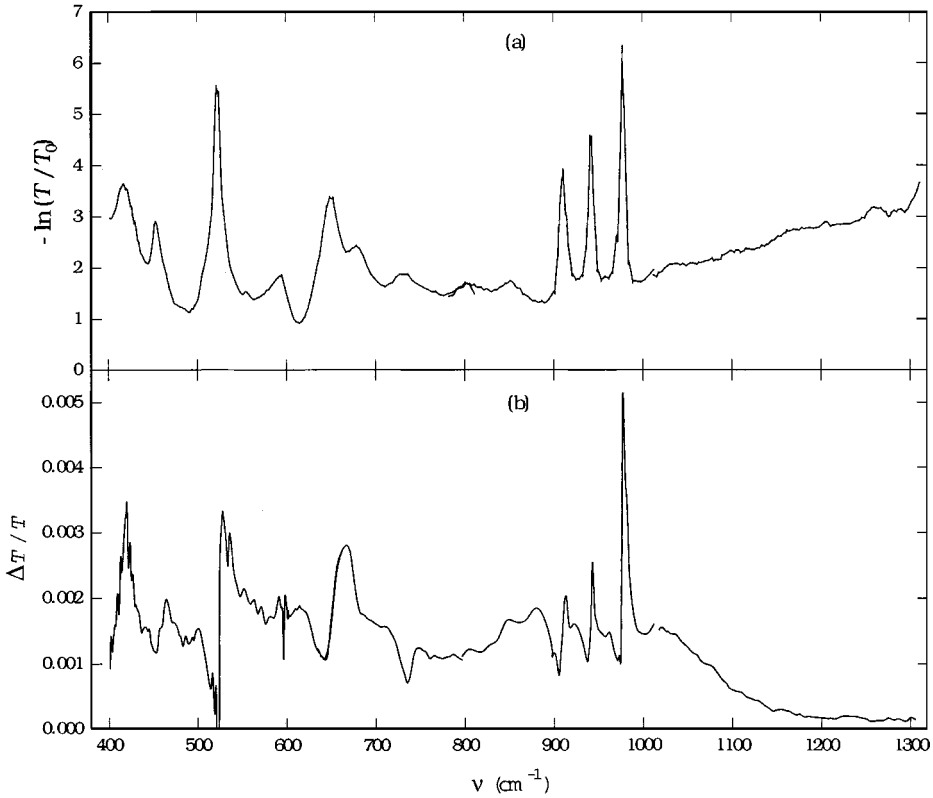

FIG. 4. (a) Optical density and (b) relative change in transmission with application of an electric field spectra for a blue bronze crystal at 82 K. The scale factor $T_0 \approx 1$. The experimental parameters are discussed in the text. The scatter in the curves indicates the uncertainty.

spectral shapes for any of these changes.) For example, Fig. 5 shows an enlarged view of the optical density and $\Delta T/T$ spectra between 400 and 575 cm^{-1}, with three strong phonon absorption lines, each changing in a different way with electric field.

For the phonon at 452 cm^{-1}, the $\Delta T/T$ spectrum has the "M" shape characteristic of a change in bandwidth. Comparison of the $\ln(T)$ and $\Delta T/T$ spectra indicates that the bandwidth changes by $\approx 0.006\ cm^{-1}$, with the linewidth decreasing when the contact is positive and increasing when negative. A few other phonons have $\Delta T/T$ spectra of this shape, all with the same polarity; the largest bandwidth change (0.03 cm^{-1}) is observed for the 733 cm^{-1} phonon (see Fig. 4) (13). These changes can be easily understood in terms of changes in quasiparticle density: at the positive contact, the decrease in quasiparticle density decreases damping of the phonon damping and its linewidth, with opposite sign changes at negative contact. Similar changes in spectra can be observed by changing the temperature of the sample by $\approx \pm 1$ K (31).

For the 522 cm^{-1} phonon, $\Delta T/T$ has a derivative line shape, indicating that the CDW polarization primarily affects the phonon frequency. Comparison of the $\ln(T)$ and $\Delta T/T$ spectra indicates that the frequency shift $\Delta\nu \approx 0.01\ cm^{-1}$, with the frequency decreasing when the contact is positive and increasing when it is negative. Most of the phonons in Fig. 4 have changes of this type, with changes of the same polarity and magnitudes varying from 0.005 to 0.03 cm^{-1} (13). The physics underlying these frequency shifts is unclear. A possibility is that the phonon mixes with virtual interband quasiparticle excitation, which would decrease the frequency of a phonon with $\nu < \nu_{gap}$. If the quasiparticle density decreases at the positive contact, it would increase the strength of this mixing, further decreasing the phonon frequency. (Opposite sign effects occur at the negative contact.) While this mechanism gives the correct sign for the observed frequency shifts, it would also predict that the electromodulated frequency shifts were activated; in fact, they have a weaker temperature dependence than the conductivity (13).

For the 418 cm^{-1} phonon, CDW polarization appears to mostly affect the oscillator strength. Its amplitude changes by $\approx 0.07\%$, decreasing (increasing) when the contact is positive (negative). This is the only phonon for which we observe a change of this type, and its underlying physics is also unclear. Rice discussed changes in the oscillator strengths of optical phonons due to mixing with a CDW (32). He explicitly considered a quasi-one-dimensional metal

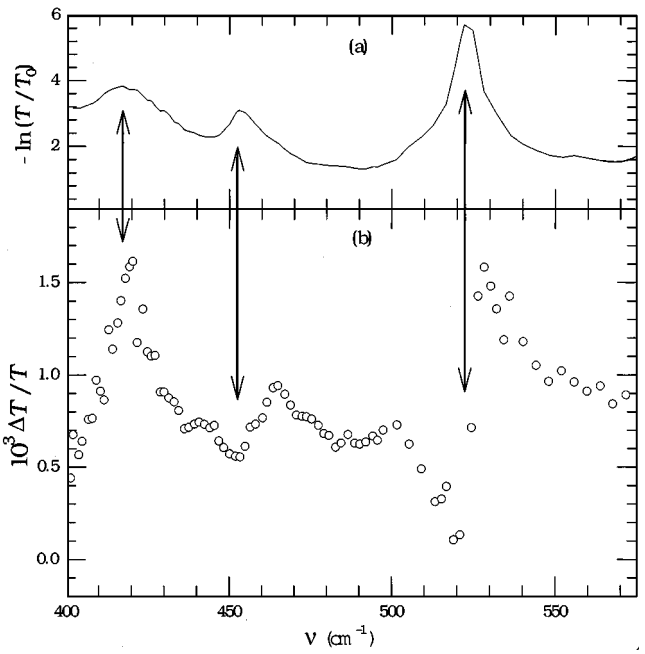

FIG. 5. Enlarged view of the low frequency portion of Fig. 4. The vertical arrows show the three phonon modes discussed in the text.

consisting of stacks of discrete molecules, for which he found that longitudinally polarized phonons would gain oscillator strength from the presence of a CDW. For the more extended structure of $K_{0.3}MoO_3$, it is possible that the phonon polarization dependence can become mixed. However, for this mechanism to apply to the polarity-dependent changes observed by us would require that CDW polarization (i.e., phase gradients) would be accompanied by (asymmetric) changes in the CDW amplitude (33).

4. CONCLUSION

Materials with sliding charge-density waves are well-known for their variety of unusual electronic transport properties. In this paper, we discussed unusual changes in the phonon spectra caused by CDW depinning.

While our recent results on low-frequency elastic properties were compared with a relaxational model (12), it is not clear how completely this model accounts for all observations. It may be that some contributions to the softening come from "instantaneous," i.e., intrinsic, phonon–CDW interactions; indeed, the interaction of the CDW polarization with optic phonons suggests that such must be the case, and a few models for this have been proposed (4, 23, 34–37). Within the context of the relaxational model, it is not clear how to account for the strong voltage dependence of the relaxation time nor the behavior of moduli at high frequencies (9). There has been no research on utilizing the large shear modulus anomalies in devices; in addition to the dynamic effects discussed here, the static modulus exhibits large hysteretic (i.e., "memory") effects (18).

While the electric field induced changes in infrared transmission are small, the very small fields needed and wide spectral response also suggest that there may be specialized applications. To date, the only material investigated has been $K_{0.3}MoO_3$, and only in transmission for transversely (i.e., [102]) polarized light. Indeed, one might expect much larger effects for light polarized along the conducting chains [010]; for this polarization, reflectivity studies are required. Understanding the variety of phonon changes observed will certainly require identification of the different modes.

ACKNOWLEDGMENTS

We are pleased to be able to contribute this paper honoring J. M. Honig for his many contributions to the science of unusual materials. We thank R. E. Thorne for providing crystals and G. Murthy for helpful discussions. Support for this research was provided by the National Science Foundation, Grants DMR-9300597 and DMR-9731257.

REFERENCES

1. C. Schlenker, J. Dumas, M. Greenblatt, and S. Van Smaalen (Eds.), *in* "Physics and Chemistry of Low-Dimensional Inorganic Conductors." Plenum, New York, 1996.
2. G. Gruner, *Rev. Mod. Phys.* **60,** 1129 (1988).
3. J. W. Brill, W. Roark, and G. Minton, *Phys. Rev. B* **33,** 6831 (1986).
4. G. Mozurkewich, P. M. Chaikin, W. G. Clark, and G. Gruner, *Solid State Commun.* **56,** 421 (1985).
5. X. D. Xiang and J. W. Brill, *Phys. Rev. B* **36,** 2969 (1987).
6. X. D. Xiang and J. W. Brill, *Phys. Rev. B* **39,** 1290 (1989).
7. A. Suzuki, H. Mizubayashi, and S. Okuda, *J. Phys. Soc. Jpn.* **57,** 4322 (1988).
8. A. J. Rivero, H. R. Salva, A. A. Ghilarducci, P. Monceau, and F. Levy, *Solid State Commun.* **106,** 13 (1998).
9. X. D. Xiang and J. W. Brill, *Phys. Rev. Lett.* **63,** 1853 (1989).
10. R. L. Jacobsen, M. B. Weissman, and G. Mozurkewich, *Phys. Rev. B* **43,** 13198 (1991).
11. X. Zhan and J. W. Brill, *Phys. Rev. B* **56,** 1204 (1997).
12. G. Mozurkewich, *Phys. Rev. B* **42,** 11183 (1990).
13. B. M. Emerling, M. E. Itkis, and J. W. Brill, *Euro. Phys. Jnl. B* **16,** 295 (2000).
14. T. Sambongi, K. Tsustsumi, Y. Shiozaki, M. Yamamoto, K. Yamaya, and Y. Abe, *Solid State Commun.* **22,** 729 (1977).
15. M. H. Jericho and A. M. Simpson, *Phys. Rev. B* **34,** 1116 (1986).
16. X. D. Xiang, J. W. Brill, and W. L. Fuqua, *Rev. Sci. Inst.* **60,** 3035 (1989).
17. M. E. Itkis, B. M. Emerling, and J. W. Brill, *Phys. Rev. B* **52,** R11545 (1995).
18. X. Zhan and J. W. Brill, *Phys. Rev. B* **52,** R8601 (1995).
19. S. Havriliak and S. Negami, *J. Polym. Sci. C* **14,** 99 (1966).
20. S. Havriliak and S. Negami, *Polymer* **8,** 161 (1967).
21. X. Zhan and J. W. Brill, *Synth. Met.* **103,** 2671 (1999).
22. O. Narayan and D. S. Fisher, *Phys. Rev. Lett.* **68,** 3615 (1983).
23. A. K. Sood and G. Gruner, *Phys. Rev. B* **32,** 2711 (1985).
24. C. Schlenker, C. Fillippini, J. Marcus, J. Dumas, J. P. Pouget, and S. Kagoshima, *J. Phys.* (*Paris*) **44**(C3), 1758 (1983).
25. L. Degiorgi, St. Thieme, B. Alavi, G. Gruner, R. H. McKenzie, K. Kim, and F. Levy, *Phys. Rev. B* **52,** 5603 (1995).

26. M. E. Itkis and J. W. Brill, *Phys. Rev. Lett*. **72,** 2049 (1994).
27. R. M. Fleming and L. F. Schneemeyer, *Phys. Rev. Lett*. **28,** 6996 (1983).
28. S. Braozovskii, N. Kirova, H. Requardt, F. Ya. Nad, P. Monceau, R. Currat, J. E. Lorenzo, G. Grubel, and Ch. Vettier, *Phys. Rev. B* **61,** 10640 (2000).
29. L. Forro, J. R. Cooper, A. Janossy, and K. Kamaras, *Phys. Rev. B* **34,** 9047 (1986).
30. S. Jandl, M. Banville, C. Pepin, J. Marcus, and C. Schlenker, *Phys. Rev. B* **40,** 12487 (1989).
31. M. E. Itkis, B. M. Emerling, and J. W. Brill, *Phys. Rev. B* **56,** 6506 (1997).
32. M. J. Rice, *Phys. Rev. Lett*. **37,** 36 (1976).
33. A. Janossy, G. Mihaly, and G. Kriza, *Solid State Commun.* **51,** 63 (1984).
34. S. Liu and L. Sneddon, *Phys. Rev. B* **44,** 3555 (1991).
35. A. Virosztek and K. Maki, *Phys. Rev. B* **53,** 3741 (1996).
36. R. Zeyher, *Phys. Rev. Lett*. **61,** 1009 (1988).
37. A. S. Rozhavsky, Yu. S. Kivshar, and A. V. Nedzvetsky, *Phys. Rev. B* **40,** 4168 (1989).